High-order harmonic generation in the tunneling regime

Kenzo Miyazaki and Hideyuki Takada
Laser Section, Optoelectronics Division, Electrotechnical Laboratory, 1-1-4, Umezono, Tsukuba, Ibaraki 305, Japan
(Received 7 November 1994; revised manuscript received 12 May 1995)

We present systematic experimental studies of high-order harmonic generation in He and Ne that have been performed with an intense, femtosecond Ti:sapphire laser at intensities in the tunneling regime, where special attention is concentrated on the strong-field effect. A broad plateau is formed in the harmonic distribution that includes harmonic peaks at low and high orders and the observed highest orders (shortest wavelengths) are the 103rd (7.6 nm) for He and 95th (8.2 nm) for Ne. The laser-ellipticity-dependent harmonics observed suggest different generation processes for the low orders below and around the atomic ionization limit and for the high orders in and above the plateau region. The medium ionization is found to induce strong self-defocusing of the incident laser beam, and its effects on the harmonic generation are studied. The results for the defocusing and the blueshifts of the harmonic spectra observed show that the generation of a higher-order harmonic requires a higher intensity in time and space. The theoretically predicted harmonic cutoff is demonstrated to agree well with experiment when we take into account the interaction intensity limited in the ionizing medium. The characteristic harmonic behaviors observed are discussed based on the interaction intensity and the propagation effect in the medium.

PACS number(s): 32.80.Rm; 42.65.Ky

I. INTRODUCTION

In recent years, extremely high-order harmonics have been observed in gaseous media at focused laser intensities more than $\sim 10^{13}$ W/cm^2, using intense ultrashort laser pulses [1–13]. For example, the generation has been reported of coherent radiation less than 8 nm [7,8,13] as well as the harmonic orders higher than 100 [4,7,8,10,12,13]. These experimental results strongly suggest that high-order harmonic generation is a promising approach to develop coherent soft-x-ray radiation sources. For this application, one of the most interesting subjects is concerned with the highest-order harmonic or the shortest wavelength to be generated at a specific laser intensity and/or wavelength [14].

In addition to the generation of very high-order harmonics, the characteristic harmonic behaviors, such as plateau formations, observed have suggested another field of nonlinear optics [15,16]. In fact, the strong laser fields used in the experiments are comparable with or in excess of the typical atomic Coulomb field of 10^8–10^9 V/cm, where the harmonic generation process is beyond the scope of conventional perturbation theory. In such a strong field, an atom undergoes multiphoton ionization and/or tunneling ionization. The ionization of atoms leads to a depletion of neutral atoms and has been considered so far as a limiting process in harmonic generation. However, Corkum [17] and Schafer and coworkers [18,19] have recently proposed that the tunneling ionization greatly contributes to the efficient generation of high-order harmonics. In this model, the high-order harmonics are produced through the following processes. An atomic electron escapes to the continuum via the tunneling ionization and the free electron created is first accelerated away from the parent ion by the laser field. As the field changes sign in the next half cycle, it returns to the ion and recombines to the atomic ground state with the emission of a harmonic photon.

Several experiments have been made to confirm this semiclassical model by observing laser-ellipticity dependences [20–22] and characteristic properties or the cutoff [23,24] of the harmonic generation and the results appear to support the alternative model of harmonic generation. At the same time, the experimental results reported so far have also suggested that the harmonic behaviors at high intensities are much more complicated than those predicted by the theory based on the single-atom response. In the tunneling regime, atoms used as the nonlinear medium are ionized very quickly [25,26] and the rapid ionization will play an important role in the harmonic generation process. For the purposes of understanding the harmonic generation in the tunneling regime, therefore, a detailed study is required on the interaction of a strong laser pulse with atoms in an *ionizing* medium.

In this paper, we report systematic experimental studies of the harmonic generation at intensities of more than 10^{15} W/cm^2, using intense femtosecond Ti:sapphire laser pulses, where our attention has been focused on the effects of strong ionization on the harmonic generation. To ensure the tunneling ionization at the high intensity, He and Ne atoms were used as the nonlinear medium. Helium is of particular interest for modeling the harmonic generation in the tunneling regime because of its simple structure and high ionization potential.

This paper consists of the following. Section II gives a brief description concerning some characteristic aspects of harmonic generation in an ionizing medium. In Sec. III the experimental apparatus and procedure are described. We present the experimental results in Sec. IV, which are concerned with the harmonic spectra and distributions at different intensities and medium pressures, the ellipticity-dependent harmonic generation at high intensity, the self-defocusing of the laser beam in the medium, and the blueshifts of the laser and harmonic spectra. The defocusing effects on harmonic generation were studied using a modified z-scan method. The results for defocusing allowed to estimate the interaction intensity limited in the ionizing medium, while the blueshifts of harmonic spectra suggest the

effective intensity for the generation of a specific order of harmonic. The harmonic cutoff and the characteristic behaviors of the high-order harmonics observed are discussed in Sec. V, based on the interaction intensity and the propagation effect in the ionizing medium.

II. BACKGROUND

A. Tunneling ionization

Ionization of atoms in a strong field is usually divided into two regimes by the adiabaticity or Keldysh parameter [27]

$$\gamma=(I_p/2U_p)^{1/2}, \tag{1}$$

where I_p is the ionization potential of an atom and U_p is the ponderomotive potential or quiver energy of an electron, which is given by

$$U_p=e^2E_0^2/4m_e\omega^2=9.337\times10^{-14}I\lambda^2 \text{ eV}, \tag{2}$$

with the peak electric field E_0 of a laser pulse at frequency ω, the electron mass m_e and charge e, the laser intensity I in W/cm^2, and the wavelength λ in μm. The Keldysh parameter can be interpreted as the ratio of the tunneling frequency $\omega_t=eE_0/(2m_eI_p)^{1/2}$ of an electron passing through the potential barrier to the laser frequency ω, i.e., $\gamma=\omega/\omega_t$. For a specific atom and a laser frequency ω, the ionization of an atom proceeds through the multiphoton ionization in the intensity region of $\gamma>1$ and through the tunneling in the region of $\gamma<1$.

For example, the femtosecond Ti:sapphire laser ($\lambda\sim782$ nm) used in the present experiments gives $\gamma\sim0.5$ at $I\sim8.6\times10^{14}$ and 7.6×10^{14} W/cm^2 for neutral He and Ne atoms, respectively. As will be described in Sec. III, we had to use a much higher intensity than these for efficient harmonic generation in He and Ne. Under experimental conditions, medium ionization through the tunneling will become significant and proceed very quickly at the beginning of a laser pulse. In a gaseous medium, the temporal change in the electron density $N_e(t)$ at time t is described by the rate equation

$$dN_e(t)=N(t)W(t,E)dt, \tag{3}$$

where $N(t)$ is the neutral atom density and $W(t,E)$ is the tunneling ionization rate depending on the field strength or the amplitude $E(t)$ at t. We can assume for He and Ne that only singly ionized ions are predominantly produced through the tunneling at the intensity concerned and the relation $N_0=N_e(t)+N(t)$ is maintained in the interaction volume, where N_0 is the initial density of neutral atoms. From Eq. (3), $N_e(t)$ increases in a laser pulse as

$$N_e(t)=N_0\left[1-\exp\left(-\int_{-\infty}^{t}W(t,E)dt\right)\right]. \tag{4}$$

The tunneling ionization rate $W(t,E)$ may be calculated using the formula (in a.u.) given by Ammosov *et al.* [28]

$$W(t,E)=(3E/\pi E^*)^{1/2}|C_{nl}|^2(2E^*/E)^{2n-|m|-1}I_pf(l,m)\times\exp(-2E^*/3E), \tag{5}$$

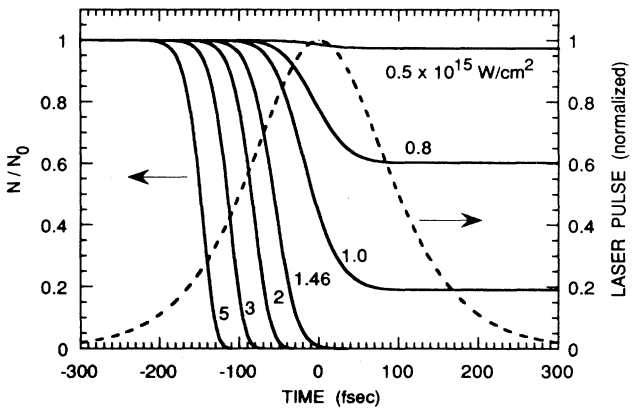

FIG. 1. Calculated temporal changes in the ratio N/N_0 through the tunneling ionization of He atoms at peak laser intensities $I_0=0.5$, 0.8, 1, 1.46, 2, 3, and 5×10^{15} W/cm^2, where N is the neutral atom density at time t and N_0 is the initial density. The incident laser pulse indicated by a dashed line is assumed to have a sech^2 shape and a FWHM of 200 fsec.

where $f(l,m)=(2l+1)(l+|m|)!/[2^{|m|}(|m|)!(1-|m|)!]$ with the orbital and magnetic quantum numbers l and m, $E^*=(2I_p)^{3/2}$, $n=Z(2I_p)^{-1/2}$ with the charge Z of a residual ion, and C_{nl} is a numerical constant on the order of 2. The ionization rate depends strongly on the field strength E.

Using Eqs. (4) and (5), we have calculated the temporal change in $N(t)/N_0$ for various values of the peak laser intensity I_0, where the laser pulse is assumed to have a sech^2 shape in time and a full width at half maximum (FWHM) of 200 fsec. The numerical results for He are shown in Fig. 1, where the temporal change in the laser intensity $I(t)$ is given for comparison. One can see a rapid increase in ionization with increasing I_0 due to the strong I dependence of $W(t)$. For example, at $I_0\sim3\times10^{15}$ W/cm^2, He atoms are completely ionized in a duration of 60–70 fsec at the beginning of a laser pulse. According to the semiclassical picture [17–19], the harmonic can be produced in this short period of a laser pulse.

With increasing I_0, the strong field may suppress the potential barrier down to a level of the atomic ground state and then the atomic electron can escape over the potential barrier to the continuum. As described by Augst *et al.* [29] and Ilkov, Decker, and Chin [30], this barrier suppression (BS) ionization restricts the tunneling ionization. Assuming a simple Coulomb field, the field E_{BS} for the BS is given by $E_{BS}\sim I_p^2/4Z$ (in a.u.), corresponding to the laser intensity $I_{BS}=1.46\times10^{15}$ W/cm^2 (or $\gamma\sim0.38$) for He and $I_{BS}=8.64\times10^{14}$ W/cm^2 (or $\gamma\sim0.47$) for Ne at $\lambda=782$ nm. As seen in Fig. 1, however, at $I_0\geqslant\sim I_{BS}$ the complete ionization of He atoms takes place through the tunneling in the leading edge of the laser pulse. This indicates that the BS ionization is never induced by the laser pulse concerned.

B. Harmonic generation in the ionizing medium

It is well known that the harmonic generation is dominated by the phase mismatch $\Delta\phi$ between the induced polarization and the generated harmonic field. In a medium

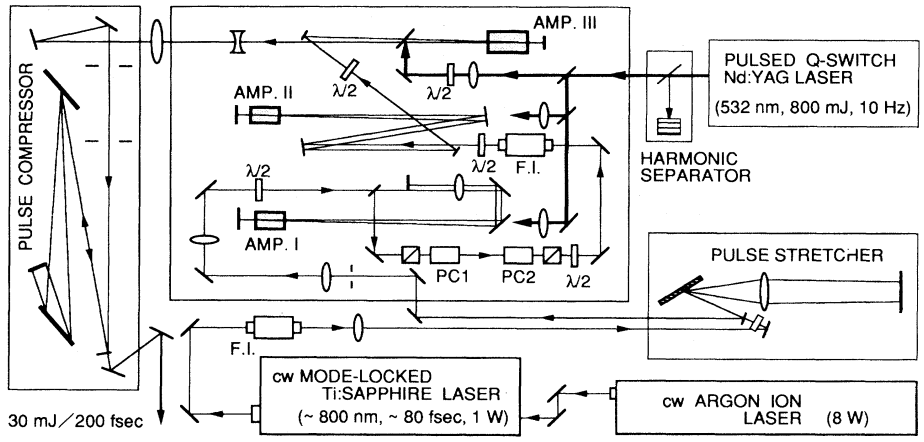

FIG. 2. Schematic diagram of the femtosecond Ti:sapphire laser amplification system used. PC1 and PC2 are the Pockels cells; FI is the Faraday isolator.

ionized by the strong field, $\Delta\phi$ for the qth harmonic generation is predominantly introduced by the focused laser beam and the medium ionization as

$$\Delta\phi=\Delta\phi_{\text{focus}}+\Delta\phi_{\text{electron}}. \tag{6}$$

The phase mismatch $\Delta\phi_{\text{focus}}$ is described as

$$\Delta\phi_{\text{focus}}=2(q-1)L/b \tag{7}$$

for a well-collimated $(b/L\gg 1)$, lowest-order Gaussian beam that is focused in a uniform medium of length L with the confocal parameter b [31]. When the ionization proceeds in time with increasing laser intensity, the refractive index of the medium is rapidly changed in a laser pulse and the resulting phase mismatch

$$\Delta\phi_{\text{electron}}=(q\omega L/c)(n_q-n_1) \tag{8}$$

due to free electrons becomes significant, where c is the speed of light and the refractive index n_q for the qth harmonic is given by

$$n_q(t)=(1-\omega_p^2/\omega_q^2)^{1/2}, \tag{9}$$

with the plasma frequency $\omega_p=(4\pi N_e e^2/m_e)^{1/2}$ in cgs and the qth harmonic frequency ω_q.

In an ionizing medium, the qth harmonic field is temporally built up coherently over the length $L_c\sim\pi/\Delta k$, where the wave-vector mismatch Δk is given by $\Delta k=\Delta\phi/L$. In the present experimental conditions described in Sec. III, the time-dependent coherence length L_c is dominated by $\Delta k_{\text{electron}}$ when more than several percent of the neutral atoms are ionized.

According to the semiclassical picture proposed [17–19], the harmonic is generated by an electron and ion pair in only one or two optical cycles after the tunneling. Then the harmonic field generated at time t is proportional to the instantaneous density $N(t)W(t,E)$ of an electron-ion pair created at t. Assuming that the role of propagation or phase matching can be separated from the single-atom contribution, the time-dependent change in the qth harmonic intensity $I(q\omega,t)$ may be approximated as

$$I(q\omega,t)\propto|d(q\omega,t)|^2N^2(t)W^2(t,E)|F_q(\Delta k,t)|^2V(t), \tag{10}$$

where $d(q\omega,t)$ is the qth harmonic dipole moment formed by an electron-ion pair, $V(t)$ is the medium volume interacting with the laser pulse, and $|F_q(\Delta k,t)|^2$ is the phase-matching factor that describes the propagation effect in the ionizing medium. In the nonperturbative regime, the phase-matching factor is a complicated integral that has to be solved numerically. L'Huillier and co-workers [15,32–34] have found that in the strong-field regime, this factor is much less sensitive to the laser intensity than in the weak-field limit. This comes from the fact that at high intensities, the dipole moment for harmonic generation varies very slowly with the laser intensity, in contrast to that in the weak-field limit. We can expect that this is also the case in the tunneling regime concerned.

According to the theoretical model [17–19] in the tunneling regime, the emitted harmonic photon energy is determined by the kinetic energy of an electron returning to the ion. The maximum kinetic energy of the returning electron is $3.17U_p$ and then the maximum photon energy $E_{\max}$ is given by

$$E_{\max}\approx I_p+3.17U_p. \tag{11}$$

This relation is known as the cutoff law for the high-order harmonic generation by the single-atom response. However, the maximum harmonic energy observed in previous experiments [9,10,23,24] is much less than the theoretical prediction. This may be attributed to the propagation effects that hide the single-atom response [23,24]. In the present study, we demonstrate that the theoretical prediction agrees well with the experimental one if we apply the laser intensity limited in the medium to estimate $E_{\max}$.

III. EXPERIMENT

The fundamental radiation used in the experiments is produced by a Ti:sapphire laser oscillator-amplifier system (Spectra Physics), which is based on the chirped-pulse amplification technique. The system configuration is schematically shown in Fig. 2. A mode-locked Ti:sapphire laser oscillator pumped by a cw (8-W) Ar ion laser generates 10-nJ,

~80-fsec seed pulses. The 80-fsec pulses are stretched to a width of 200 psec in a pulse stretcher consisting of a grating, an achromatic lens, and a total reflector. The stretched pulses are sent to the three-stage Ti:sapphire amplifiers, which are pumped by a frequency-doubled Q-switched Nd:YAG laser (where YAG denotes yttrium aluminum garnet) operating at a repetition rate of 10 Hz. After four-pass amplification in the first amplifier (AMP. I), a single pulse is electro-optically selected by using two Pockels cells. In the second (AMP. II) and third amplifiers (AMP. III), double-pass amplification is used. The output pulse energy from AMP. III is 70 mJ.

Before recompressing the amplified pulses in the double-pass grating compressor, the output beam of about 6 mm in diameter from AMP. III is expanded to a diameter of ~20 mm in order to avoid damage of optical components that constitute the compressor. In the pulse compressor, more than 50% of the pulse energy is lost due to the low diffraction efficiency of gratings. The final output from this laser system is 30 mJ in the pulse width (FWHM) of 200 fsec, corresponding to the peak power of 0.15 TW. The compressed pulse measured with a slow-scan autocorrelator is much longer than that of the oscillator pulses, due most likely to the bandwidth narrowing and additional group velocity dispersion introduced in the amplification stages. The output wavelength is centered at 782 nm with a spectral width (FWHM) of about 6 nm. Throughout the experiments, the laser output was fixed at this wavelength.

The experimental arrangement for the harmonic generation was the same as that in our previous studies [3,11,13]. Briefly, the linearly polarized Ti:sapphire laser output was focused with a 25-cm focal-length CaF_2 lens into a supersonic He or Ne beam that was synchronously jetted at 10 Hz through a modified 1-mm-diam nozzle attached on a commercial pulsed gas valve.

The focused-beam waist diameter was measured to be $2w_0 \approx 45$ μm at a very low intensity, which corresponds to the confocal parameter of $b = 4.1$ mm, assuming the lowest-order Gaussian beam. The peak laser intensity I_0, defined by the value expected in vacuum in this paper, is estimated by the relation $I_0 = 2E_{\text{pulse}}/(\tau_p \pi w_0^2)$ with the pulse energy E_{pulse}, the pulse width τ_p, and the spot size w_0. The uncertainty in I_0 was within $\pm 50\%$. The laser pulse energy used in the harmonic generation experiments was limited to ~6 mJ by inserting a diaphragm of ~8.5 mm diameter in front of the focusing lens and then I_0 was restricted to be 3.8×10^{15} W/cm^2. Higher intensities never improved the harmonic generation properties due mainly to the strong ionization and resulting defocusing of the laser beam in the gas jet. For the experiment at different laser intesities, the laser output was varied using a half-wave plate coupled with a thin-film polarizer.

To evaluate the number density of He or Ne atoms in the gas jet, we observed and compared visible fluorescence emitted by irradiating the laser pulse on the gas jet and the gas filled in a cell at various static pressures. In this measurement, I_0 was made as low as possible to minimize the defocusing effect. The gas density obtained was also compared with that calculated from the backing pressure and the nozzle configuration for the gas jet. Both were in agreement within a factor 2.

The generated harmonic radiation was detected by a windowless Cu-BeO electron multiplier (Hamamatsu R595) mounted on a 1-m grazing incidence monochromator (Minuteman 310-G) having an Au-coated 600-grooves/mm grating blazed at 5 nm. The entrance slit of the monochromator was set at a distance of 25 cm apart from the gas jet and the vertical height of the slit was fixed at 5 mm. The exit slit width of 30–200 μm was used, depending on the experimental conditions. This monochromator is useful for detecting harmonics higher than 13th order of the 782-nm laser. The harmonic signal detected was processed by a boxcar averager and recorded on a chart recorder. The wavelength dependence of detection sensitivity for the whole system has been calibrated in our previous studies [3,11].

Ions produced through the ionization were detected by a simple charge collector placed in the downstream of the gas jet. With this simple system, we could monitor both He and Ne ion signals at laser intensities higher than $I_0 \sim 3 \times 10^{14}$ W/cm^2.

IV. RESULTS

A. Harmonic spectra and distributions

A typical example of the harmonic spectra observed for He is shown in Fig. 3, where the spectral peaks are labeled by the harmonic order and small unmarked peaks are the second-order diffractions from the grating. In recording the spectrum, the entrance slit width was fixed to 30 μm, while the exit slit width was set to 60–120 μm, depending on the observed spectral range and the grating scan speed.

We found that in an identical extreme ultraviolet spectral range, the harmonic signal was much smaller than those observed in our previous experiments using visible dye and XeCl lasers [3,11]. The results obtained with three different kinds of femtosecond lasers have shown that the harmonic yield decreases with increasing the laser wavelength, while the harmonic order to be detected increases with an increase in the wavelength. In the present experiment, the highest-order harmonic (shortest wavelength) detected was the 103rd (7.6 nm) for He and the 95th (8.2 nm) for Ne.

Figure 4 shows the calibrated harmonic distributions obtained for (a) He and (b) Ne at different laser intensities. For He, with an increase in the harmonic order, the harmonic signal increases and reaches a peak around the 17th–21st orders. The harmonic order of this first peak was almost independent of the I_0 used and the peak is followed by a broad plateau where the harmonic signals are within about an order of magnitude. With increasing I_0, the harmonics in the plateau saturate quickly and only the higher orders increase to extend the plateau. At the highest intensity in Fig. 4(a), the second peak or an enhancement around the 75th–83rd orders is formed and then the higher harmonics decrease rapidly with an increase in the order. (We tentatively regard the end of the plateau as the cutoff.) The second peak around the cutoff started to appear at $I_0 \geqslant \sim 1.6 \times 10^{15}$ W/cm^2 and almost saturated at $I_0 > \sim 2 \times 10^{15}$ W/cm^2. This harmonic distribution having the second peak was found not to change with a further increase in I_0, while the harmonic signal at each order increased slightly.

For Ne, as shown in Fig. 4(b), the harmonic distributions observed represent the characteristic features similar to those for He. At $I_0 \geqslant \sim 1.7 \times 10^{15}$ W/cm^2, with an increase in the

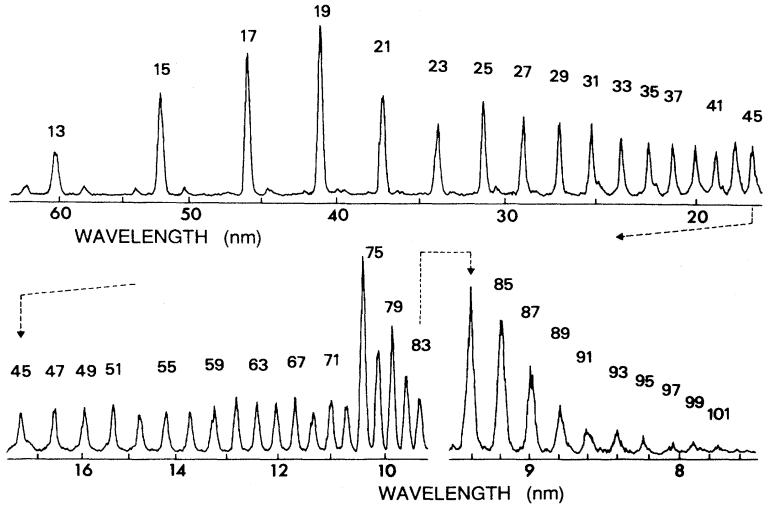

FIG. 3. Example of the high-order harmonic spectrum observed in 150-Torr He at $I_0 = 3.0 \times 10^{15}$ W/cm^2. The spectral peaks are labeled by the harmonic order, whereas the unmarked peaks are the second-order diffractions from the grating.

harmonic order, the signal is peaked at the 17th–19th orders and goes into a plateau region having a very constant yield of harmonics. It is shown more clearly in Fig. 4(b) that the harmonic cutoff moves to higher orders with increasing I_0. The enhancement around the cutoff is not as pronounced for Ne as for He. Note that the harmonic distributions were observed at a lower density of Ne by about an order of magnitude than that of He.

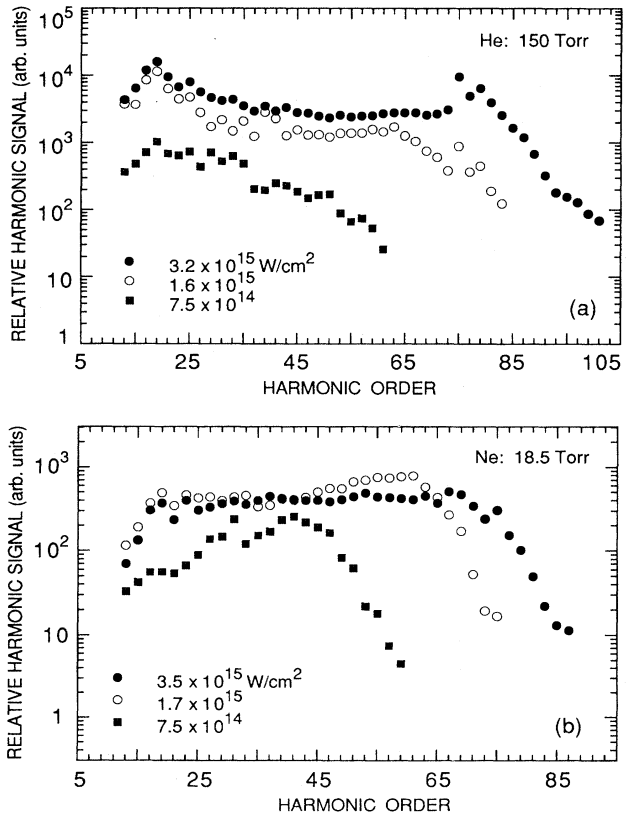

FIG. 4. Harmonic distributions observed at different laser intensities for (a) 150-Torr He and (b) 18.5-Torr Ne.

Figure 5 shows the I_0-dependent signal of the high orders around the cutoff in He. The higher-order harmonic increases more rapidly with an increase in I_0 and all the orders tend to saturate at $I_0 > \sim 2 \times 10^{15}$ W/cm^2. We have also measured the high-order harmonic signals as a function of the pressure p of He at the high intensity and the results are shown in Fig. 6. With increasing p, the 71st and 75th harmonics in the plateau increase monotonically, whereas the 89th and 91st orders above the cutoff saturate quickly. This is due most likely to the propagation effect, as will be discussed in Sec. V.

To see in more detail the effect of medium density N_0, the harmonic distributions of high orders around the cutoff were measured at different gas pressures and the results are shown in Figs. 7(a) and 7(b) for He and Ne, respectively. For both He and Ne, the harmonic cutoff appears to extend to higher orders with decreasing p, although the cutoff becomes less pronounced. For He, the harmonics less than $\sim$ the 85th order increase with an increase in p, while the higher orders and their distribution are almost independent of p. For Ne, similar behaviors of the harmonics are also ob-

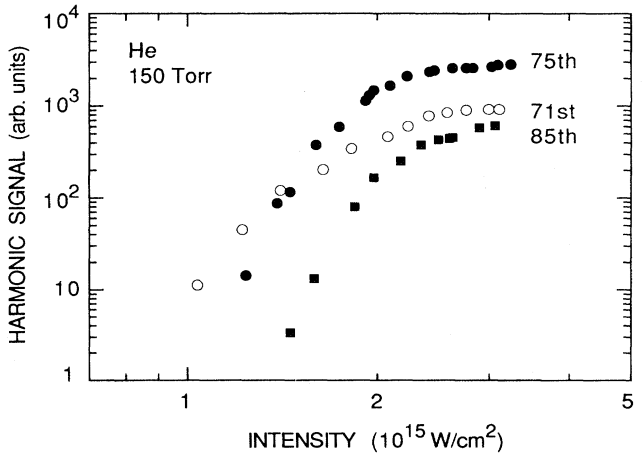

FIG. 5. High-order harmonic signals observed for 150-Torr He as a function of the laser intensity.

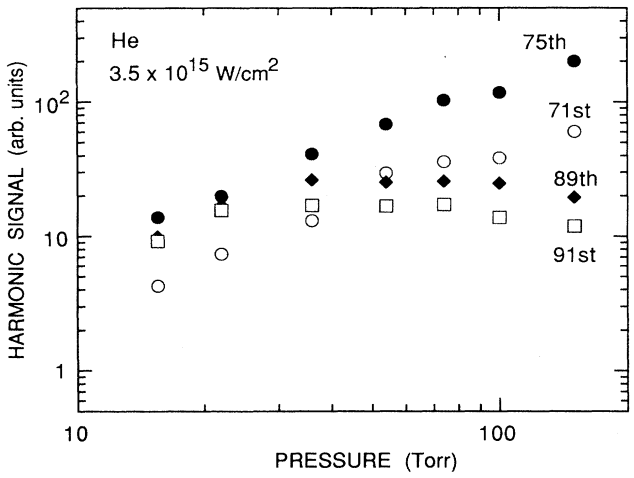

FIG. 6. High-order harmonic signals observed at $I_0=3.5\times10^{15}$ W/cm^2 as a function of the He pressure.

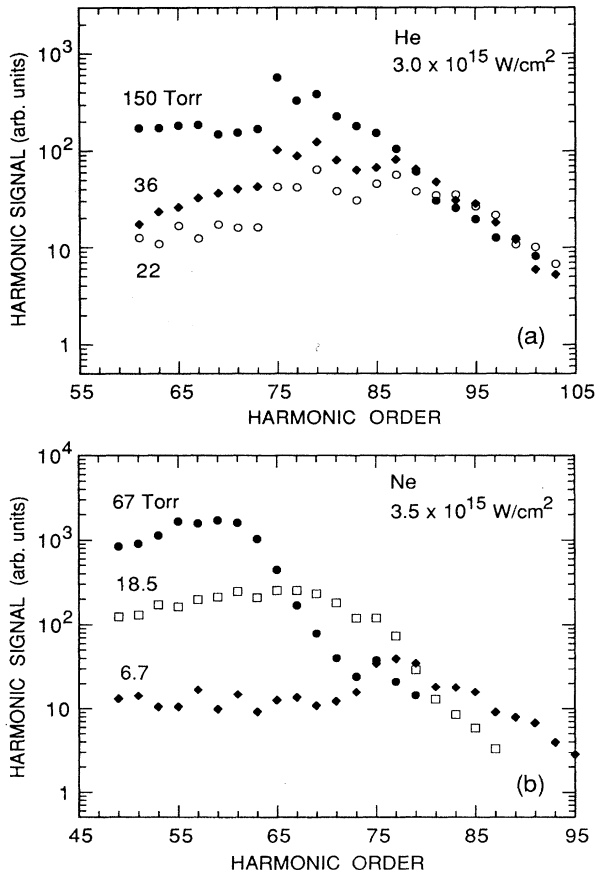

FIG. 7. Harmonic distributions observed at different gas pressures for (a) He at $I_0=3.0\times10^{15}$ W/cm^2 and (b) Ne at $I_0=3.5\times10^{15}$ W/cm^2.

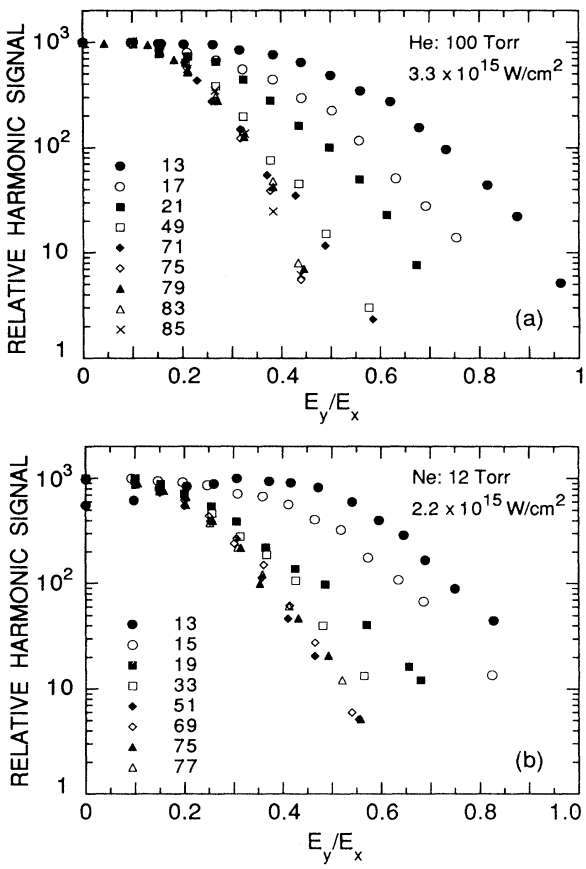

FIG. 8. Harmonic signals observed in (a) 100-Torr He at $I_0=3.3\times10^{15}$ W/cm^2 and (b) 12-Torr Ne at $I_0=2.2\times10^{15}$ W/cm^2 as a function of the ellipticity. The signal peak of each order is normalized to 10^3.

served. The harmonics generated by the coherent process should in principle have some gain with an increase in the medium density N_0. However, as shown in Figs. 6 and 7, the usual N_0^2 dependence expected in harmonic generation is not observed at the high intensity. As suggested by Eq. (10), the density dependence should be considered by $N^2(t)W^2(t,E)$, which depends on the laser intensity $I(t)$ at time t. This would destroy the conventional N_0^2 dependence in harmonic generation.

B. Ellipticity dependence

As briefly mentioned in Sec. I, theory predicts that harmonic generation in the tunneling regime is described well by the semiclassical model [17–19]. This model also suggests that the harmonic generation is very sensitive to the laser ellipticity. The ellipticity-dependent harmonic generation in He and Ne at $I_0\sim10^{15}$ W/cm^2 has been reported so far [20–22] and the results appear to support the theoretical prediction.

For the purposes of the systematic study of harmonic generation in the tunneling regime, we also measured the ellipticity dependence. The ellipticity was introduced by rotating a zeroth-order quarter-wave plate centered at 780 nm. Figure

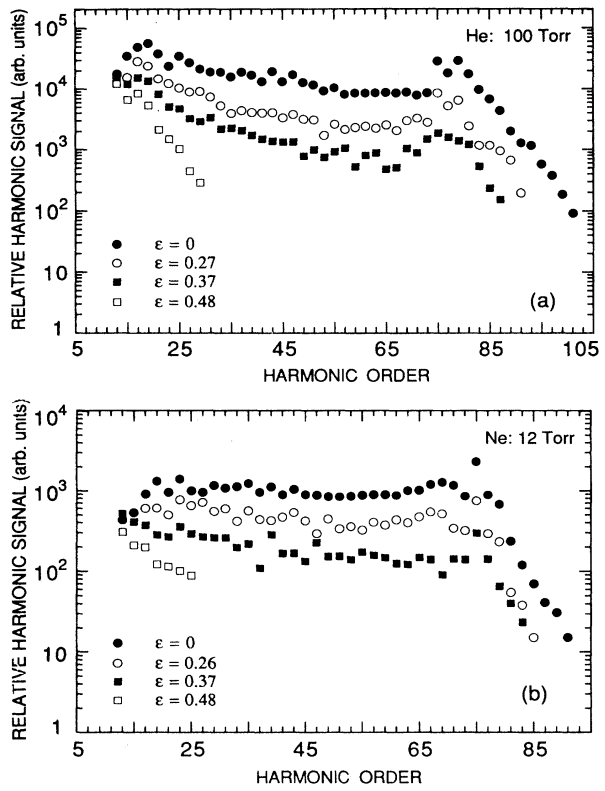

FIG. 9. Harmonic distributions observed at different ellipticities for (a) 100-Torr He at $I_0 = 2.4 \times 10^{15}$ W/cm^2 and (b) 12-Torr Ne at $I_0 = 2.2 \times 10^{15}$ W/cm^2.

8 shows the results observed for (a) He and (b) Ne, where $\varepsilon = E_y/E_x$ is the ratio of the y component to the x of the laser electric field E and then $\varepsilon = 0$ and 1 denote the linearly and circularly polarized light. The ε dependences observed seem to be less sensitive than those observed so far [20–22]. This is due most likely to the higher intensity used, at which the harmonics are almost saturated, as seen in Figs. 4 and 5. In the present experiment, the high intensity was necessary to ensure a large dynamic range of the signal for the high orders around and above the cutoff.

In Fig. 8(a), the 13th, 17th, and 21st orders for He represent a relatively weak dependence on ε, while the 49th–85th orders in the plateau decrease more rapidly with an increase in ε. Note that the ε dependences of the 75th–85th orders around the cutoff are almost independent of the harmonic order. Similar ε dependences of low- and high-order harmonics are also observed for Ne, as shown in Fig. 8(b): The 13th, 15th, and 19th orders have relatively weak dependences on ε; the 33rd–77th orders in the plateau show a fast decrease with an increase in ε; the 51st–77th orders are almost independent of the order. The order independence in the ε-dependent high-order harmonic generation has also been observed so far in Ne by Budil *et al.* [20].

In the perturbative regime, the harmonic generation also depends on the ellipticity, in which higher orders decrease more rapidly with increasing ε [20,35]. In contrast to this, almost the same ε dependence of the high orders in and above the plateau region may be a signature of the generation through the nonperturbative process. The characteristic behavior of the ε-dependent high-order harmonic generation will be discussed in more detail in Sec. V.

We note that in Fig. 8(b), the 13th order observed in Ne represents an anomalous dependence on the small value of ε ($<\sim 0.5$). The 13th order increases with increasing ε and has a broad peak at $\varepsilon \approx 0.3$–0.4. One may attribute this behavior of the 13th order to a different process of its generation. The semiclassical mode [17–19] associated with the tunneling ionization and recombination predicts the generation of harmonics having energies in excess of the ionization potential I_p. Therefore, this model cannot be applied to the generation of the 13th-order harmonic (20.6 eV) that is produced from the energy region below the Ne ionization potential (21.6 eV). We tentatively assume that the 13th order is generated by neutral Ne atoms. Then the 12 laser photons, each of which has a bandwidth of ~ 6 nm, can be in resonance with the $2p^5 3p$ states of Ne and the 13 photons with the $2p^5 5s$ states. The introduction of ellipticity opens a new channel for 13th-order harmonic generation through the process consisting of the 12 linearly polarized photons plus a single circularly polarized photon. Because of the angular-momentum conservation for the dipole transition, the 13th-order harmonic generated by this process would be circularly (or elliptically) polarized. The circularly polarized 13th-order harmonic can increase to some extent with an increase in ε, while the linearly polarized 13th order decreases with increasing ε. Thus the ε-dependent 13th-order signal would be peaked by a partial introduction of the circularly polarized component. Because of the resonant enhancement, the harmonic generation through the new channel is expected to be efficient. When the incident high-intensity field shifts the excited states to a higher energy by the ac Stark effect [36], one can expect additional resonance enhancement [3,11,37] through the $2p^5 4d$ and other excited states of Ne atoms.

In He, the photon energies of the 13th and 15th orders (23.8 eV) are smaller than the ionization potential (24.6 eV), but we never observed such an anomalous ε dependence as in Ne. This is likely due to the fact that neither the 12- nor the 14-photon resonance for the new channel can be expected for He at the present laser wavelength. Recently, Burnett, Kan, and Corkum [38] have observed a similar anomalous ε dependence of the 13th-order harmonic in Ne with a femtosecond Ti:sapphire laser at $\lambda \sim 775$ nm. From the observed polarization direction of the 13th-order harmonic, they have proposed a change in mechanism predominantly responsible for the harmonic generation from the free-bound to the free-free transition via tunneling ionization. However, this mechanism does not account for the present results for He that the 13th and 15th orders do not represent any dip at $\varepsilon = 0$.

Figure 9 shows the harmonic distributions observed at different ellipticities for (a) He and (b) Ne. The distribution at $\varepsilon = 0$ is basically the same as that observed at the highest intensity in Fig. 4. As expected from the results shown in Fig. 8, the high-order harmonics in and above the plateau region decrease rapidly with increasing ε. However, the harmonic distributions for both He and Ne are not greatly modified by increasing the ellipticity up to $\varepsilon \approx 0.37$. This indicates that for ellipticity less than $\varepsilon \approx 0.37$, the linearly polarized component of the laser pulse is still intense enough to satu-

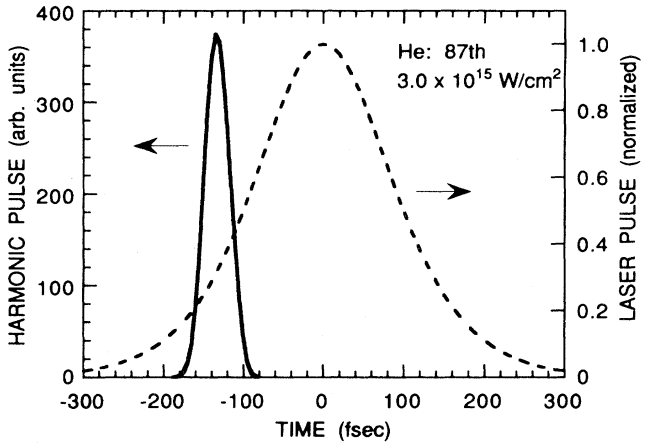

FIG. 10. Calculated temporal change in the 87th-order harmonic for 150-Torr He at $I_0=3.0\times10^{15}$ W/cm^2. The laser pulse indicated by the dashed line is the same as in Fig. 1.

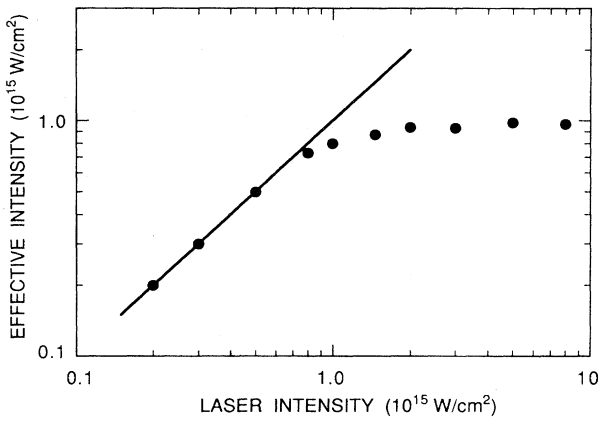

FIG. 11. Calculated effective intensity for the 87th-order generation in 150-Torr He as a function of the peak intensity I_0. The solid line indicates the slope of unity.

rate the high-order harmonics, as shown in Fig. 5. In fact, at $\varepsilon=0.37$ in Fig. 9(a), the linearly polarized component is $I_0(1-\varepsilon^2)/(1+\varepsilon^2)\sim1.8\times10^{15}$ W/cm^2, which is close to the intensity for saturation of the harmonics in the plateau, as discussed above. Nevertheless, the harmonic yield is greatly reduced by the ellipticity. This strongly suggests that the ellipticity restricts significantly the tunneling electrons from returning to the parent ions.

In contrast to the high orders, the low orders shown in Fig. 9, especially those below the first peak in the distribution, are much less affected by the ellipticity. As shown in Fig. 4, the low-order harmonics maintain the saturated feature at $I_0>\sim1.6\times10^{15}$ W/cm^2. If the low orders are generated by the same process as the high orders, they should also be quenched significantly by the ellipticity. Taking into account the characteristic nature of the 13th order in Ne, we may conclude that the low orders below the first peak are predominantly produced by the nonlinear response of atomic electrons. Then the first peaks at low orders observed in the harmonic distributions may be attributed to the resonance enhancement due to the ac Stark shifts of the excited states, as discussed in our previous studies [3,11].

C. Harmonic pulse

It is clear that the cutoff law given by Eq. (11) does not hold for the results shown in Figs. 4 and 7 when I_0 is used to estimate $E_{\max}$. When I_0 is so high as to quickly ionize the medium, as suggested by the result shown in Fig. 1, the laser intensity $I(t)$ for the most efficient harmonic generation would be certaintly limited to a lower value than I_0 due to the rapid decrease in $N(t)/N_0$. To see the ionization effect, we made a simple calculation of the temporal change in the harmonic pulse. For simplicity, we replace $F_q(\Delta k,t)$ in Eq. (10) by the coherence length $L_c\approx\pi L/(\Delta\phi_{\text{focus}}+\Delta\phi_{\text{electron}})$, which is calculated using Eqs. (7) and (8). With this replacement, we consider the harmonic generation from a time-dependent single coherence length in the ionizing medium. Furthermore, we assume a constant value for the qth harmonic dipole moment $d(q\omega)$ in Eq. (10). This assumption for $d(q\omega)$ might be a rough approximation in the strong-field regime concerned where $d(q\omega)$ varies very slowly with the laser intensity [23,39,40]. The primary failing of the present simple calculation is that we do not have the relative harmonic strength among different orders and the detailed nature of the propagation effect in the medium. However, the calculated results may allow us to see the most characteristic features of harmonic generation in an ionizing medium. [The detailed treatments of $F_q(\Delta k,t)$ and $d(q\omega)$ in the strongly ionizing medium are beyond the scope of this paper.]

Figure 10 shows an example of the calculated time-dependent change of the 87th-order harmonic in 150-Torr He at $I_0=3\times10^{15}$ W/cm^2. Corresponding to the results shown in Fig. 1, the harmonic pulse is produced only in a short temporal region at the beginning of the laser pulse. The harmonic peak that is seen at $t\sim-140$ fsec is predominantly originated by the maximum production rate of electron and ion pairs through the tunneling rather than by the temporal change in L_c.

We define the *effective intensity* I_q for the qth-order harmonic generation by the laser intensity $I(t)$, which gives the harmonic peak at t in a laser pulse. In Fig. 10, I_q is $\sim9\times10^{14}$ W/cm^2, where only several percent of the 150-Torr He is found to be ionized by referring to Fig. 1. Figure 11 shows the calculated I_q for the 87th-order generation in He as a function of I_0. The result indicates that I_{87} never exceeds $\sim1\times10^{15}$ W/cm^2 with an increase in I_0 up to $\sim1\times10^{16}$ W/cm^2, while the 87th-order harmonic peak has been found to increase with increasing I_0.

D. Blueshifts

Experimentally, the effective intensity I_q defined above depends on the whole processes of harmonic generation, as given by Eq. (10), and may be evaluated from blueshifts of laser and/or harmonic spectra in an ionizing medium. The spectral blueshift is induced by the time-dependent phase or refractive-index change caused by $\partial N_e/\partial t$ [41–44]. Several authors have observed the shifts of harmonic spectra and discussed the harmonic generation in the ionizing medium

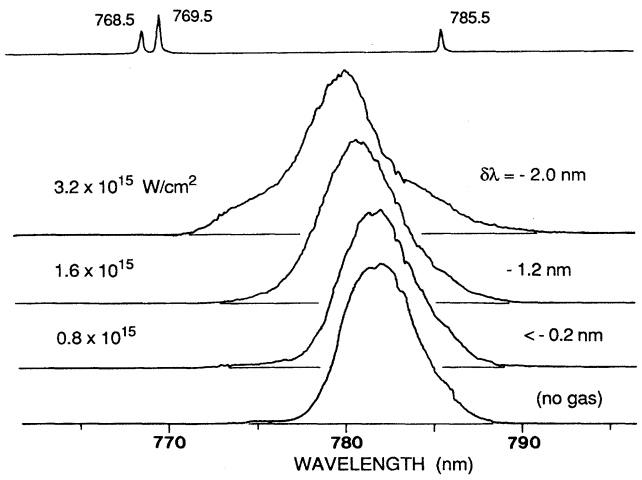

FIG. 12. Laser spectra after interaction with the 150-Torr He jet at $I_0=0.8$, 1.6, and 3.2×10^{15} W/cm^2. The lowest is the nonshifted laser spectrum and the top is the reference spectrum from a Kr discharge.

[7,24], but no attempt has been made, as far as we know, to estimate I_q for the qth-order harmonic generation.

Using Eq. (9), the shift $\delta\lambda$ of the laser spectrum is obtained as [41]

$$\delta\lambda=-(e^2\lambda^3/2\pi m_e c^3)L\partial N_e(t)/\partial t. \tag{12}$$

We can reasonably assume that $\delta\lambda$ leads to the shift $\delta\lambda_q=\delta\lambda/q$ of the qth-order harmonic spectrum at $\lambda_q=\lambda/q$ [24,44]. The harmonic spectrum can also be shifted due to the refractive index change at λ_q, but this shift, given by $\delta\lambda_q=\delta\lambda/q^3$, is much smaller than $\delta\lambda/q$. (Hereafter we describe and discuss the shifts by absolute values, i.e., $\delta\lambda\equiv|\delta\lambda|$ and $\delta\lambda_q\equiv|\delta\lambda_q|$.)

We observed the laser spectrum using an optical multichannel analyzer that was attached on the exit slit of a 20-cm focal-length spectrometer, while the harmonic spectra were observed by scanning very slowly the grazing incidence monochromator. In Fig. 12 the I_0-dependent laser spectrum observed for He is shown. With increasing I_0, the laser spectrum shifts to a shorter wavelength, as expected. For 150-Torr He, the largest shift observed is $\delta\lambda=2.0$ nm at $I_0=3.2\times10^{15}$ W/cm^2. This value of $\delta\lambda$ is very close to those observed by Macklin, Kmetec, and Gordon [7] for 24-Torr Ne and Wahlström *et al.* [24] for 20-Torr Xe with femtosecond Ti:sapphire laser pulses. Figure 13 shows the I_0-dependent harmonic spectra for the 15th and 29th orders generated in 150-Torr He. The nonshifted peaks of harmonic spectra are identified as those observed at the lowest intensity $I_0=6.8\times10^{14}$ W/cm^2, at which no fundamental shift was observed, as shown in Fig. 12. With increasing I_0, the harmonic shift $\delta\lambda_q$ increases and the width of the spectrum becomes broader.

Comparing with the results shown in Figs. 12 and 13, we note that $\delta\lambda_q$ is much larger than $\delta\lambda/q$. For example, the shift $\delta\lambda_{15}=0.32$ nm observed for the 15th order at $I_0=2.8\times10^{15}$ W/cm^2 has to originate from $\delta\lambda=4.8$ nm, but the observed $\delta\lambda$ is only 2 nm at $I_0=3.2\times10^{15}$ W/cm^2. This

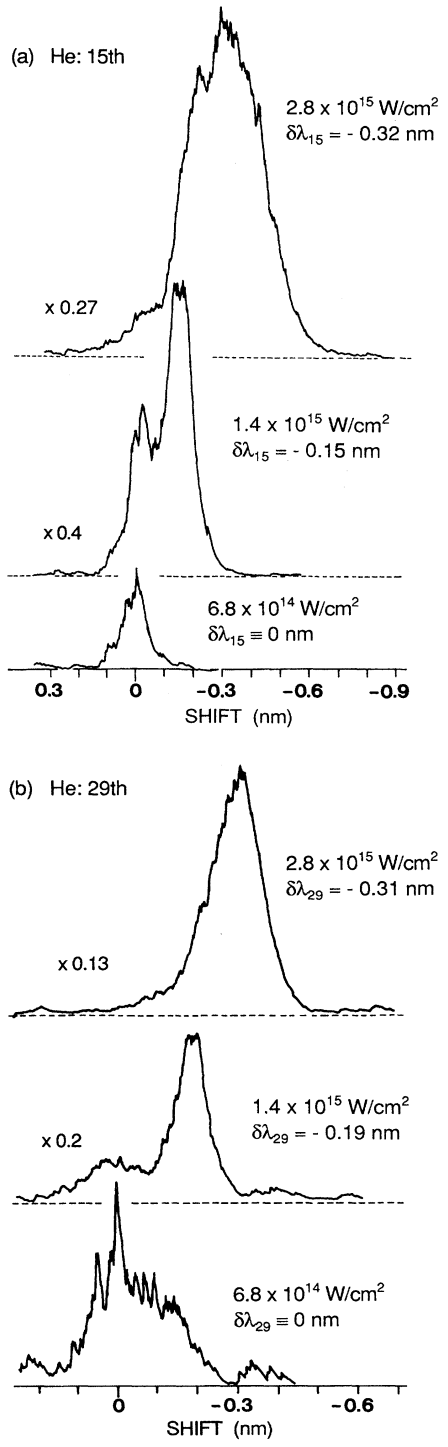

FIG. 13. Harmonic spectra of (a) the 15th and (b) the 29th orders observed for 150-Torr He at $I_0=0.68$, 1.4, and 2.8×10^{15} W/cm^2. The nonshifted peaks of the harmonic spectrum are identified as those observed at the lowest intensity.

is expected in the following situation. According to the theoretical model [17–19], harmonic generation is expected only in a limited temporal region where the medium ionization proceeds, as seen in Figs. 1 and 10. In this limited temporal

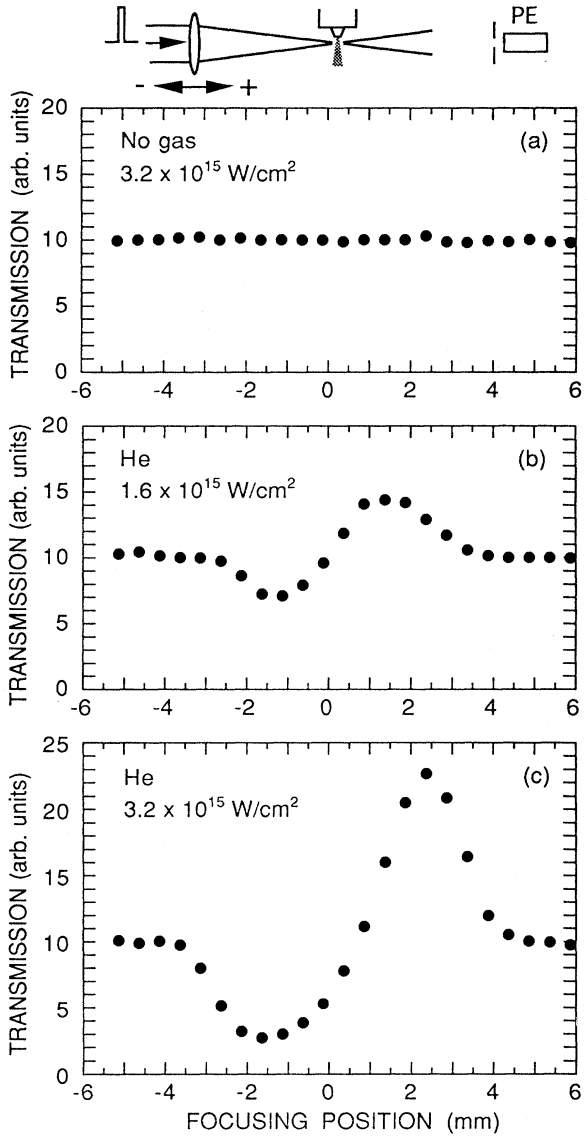

FIG. 14. Laser pulse energy transmitted through an aperture as a function of the position of laser focus in the presence of (a) no gas jet at $I_0=3.2\times10^{15}$ W/cm^2, (b) a He jet of 150 Torr at $I_0=1.6\times10^{15}$ W/cm^2, and (c) a He jet of 150 Torr at $I_0=3.2\times10^{15}$ W/cm^2. The transmission signal in the presence of no gas jet is normalized to 10 at each scan. The experimental configuration with a detector (PE) is illustrated at the top, where the distances from the gas jet to the focusing lens and to the aperture are 25 and 70 cm, respectively.

region, the laser spectrum is shifted to a shorter wavelength by an amount $\delta\lambda\approx q\,\delta\lambda_q$. However, this large shift would be averaged over a laser pulse duration and could not be detected in the time-integrated laser spectrum.

In addition to the result of $\delta\lambda_q > \delta\lambda/q$, the rapid increase in $\delta\lambda_q$ with increasing I_0 certainly demonstrates that the harmonics are generated in a limited temporal region of the high-intensity laser pulse. If the 15th- and 29th-order harmonics are generated simultaneously in the same temporal region of a laser pulse, one must have $\delta\lambda_{15}\times15\approx\delta\lambda_{29}\times29$. However, Fig. 13 shows that $\delta\lambda_{15}\times15$ is much smaller than $\delta\lambda_{29}\times29$. This result suggests that the instantaneous laser intensity $I(t)$ or the effective intensity I_{29} for the 29th-order generation is higher than I_{15} for the 15th order. This is consistent with the well known fact that a higher laser intensity is required to generate a higher-order harmonic. The observed blueshifts indicate that this is also the case for the temporal evolution of the harmonic generation.

From the observed shifts, one can estimate the effective intensities I_{15} and I_{29}. The shift $\delta\lambda_{15}=0.32$ nm in Fig. 13 results from $\delta\lambda=4.8$, as mentioned above. From Eq. (12), this value of $\delta\lambda$ gives $\partial[N_e/N_0]/\partial t=-\partial[N/N_0]/\partial t\sim1.4\times10^{12}$ sec^{-1} for a medium length of $L=0.1$ cm at a He pressure of 150 Torr, which corresponds to a decrease in N/N_0 at a rate of 14% in a 100-fsec period of the laser pulse. Similarly, $\delta\lambda_{29}=0.31$ nm is equivalent to $\delta\lambda=9.0$ nm, which leads to $\partial[N_e/N_0]/\partial t=-\partial[N/N_0]/\partial t\sim2.6\times10^{12}$ sec^{-1} or a 26% decrease in N/N_0 in a 100-fsec period. Referring to the numerical result shown in Fig. 1, the rates of $\sim1.4\times10^{12}$ and 2.6×10^{12} sec^{-1} are obtained at $I(t)=I_{15}\sim6\times10^{14}$ W/cm^2 and $I_{29}\sim7\times10^{14}$ W/cm^2, respectively, for the laser pulse of $I_0\sim3\times10^{15}$ W/cm^2. Note that no appreciable shift is produced by the laser pulse at $I_0\approx(6-7)\times10^{14}$ W/cm^2, as shown in Fig. 12, due to the slow temporal change in N/N_0. For the laser pulse of $I_0\sim3\times10^{15}$ W/cm^2, N_0 in 150-Torr He is decreased by only 3–5 % at $I(t)=(6-7)\times10^{14}$ W/cm^2.

From the results of $\delta\lambda_q$ observed at $I_0\sim1.4\times10^{15}$ W/cm^2 in Fig. 13, we have almost the same values of $I_{15}\sim6\times10^{14}$ W/cm^2 and $I_{29}\sim7\times10^{14}$ W/cm^2. This indicates that at $I_0\gg I_q$, I_q for the qth-order harmonic generation is almost independent of I_0. Furthermore, the result of $I_{29}>I_{15}$ suggests that the generation of the 29th order is delayed from that of the 15th. Referring to the result shown in Fig. 1, this delay is found to be only 5–10 fsec because of the rapid decrease in N/N_0 at the high intensity.

The blueshifts of the laser and harmonic spectra were also measured for Ne. For example, $\delta\lambda=2.1$ nm and $\delta\lambda_{29}=0.31$ nm were observed for 18.5-Torr Ne at $I_0=3.2\times10^{15}$ W/cm^2. Due to the larger ionization rate of Ne atoms than that of He, the lower Ne pressure is found to induce shifts comparable to those in He.

E. Self-defocusing

In an ionizing medium, the spatial change in N_e and the resulting refractive index change is known to induce self-defocusing of the incident laser beam [45–48]. When the laser beam has a spatial intensity distribution such as the Gaussian, the medium starts to be ionized on the optic axis. The ionization or the free electrons produced reduce the refractive index of the medium along the radial direction and then the ionizing medium works as a negative lens for the incident laser beam. This self-defocusing will limit the laser intensity in the ionizing medium to a value much lower than I_0 and modify the interaction volume for the harmonic generation. Recently, we have discussed the defocusing effect on harmonic generation in order to understand the asymmetric shape of harmonic signals observed as a function of the laser

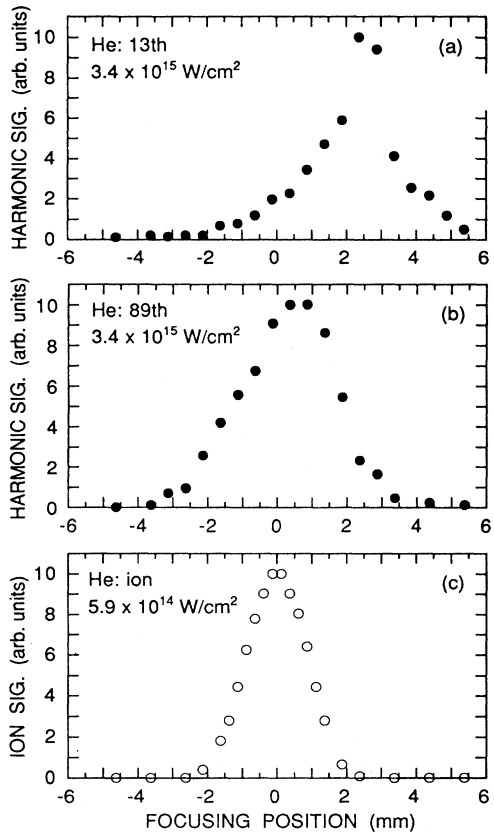

FIG. 15. (a) The 13th- and (b) the 89th-order harmonic signals observed for 150-Torr He at $I_0 = 3.4 \times 10^{15}$ W/cm^2 and (c) the ion signal detected for 3-Torr He at $I_0 = 5.9 \times 10^{14}$ W/cm^2 as a function of the position of laser focus. The signal peak is normalized to 10 at each scan. The center of the gas jet is identified by the peak ion signal.

focus with femtosecond dye and XeCl lasers [49]. However, the self-defocusing itself has not been observed so far in high-order harmonic generation.

In the present experiment, the self-defocusing in a gas jet was observed using a modified z-scan method that was similar to that developed for measurements of nonlinear properties of optical materials [50]. Focusing the Ti:sapphire laser beam into the gas jet, we detected the pulse energy transmitted through a 5-mm-diam aperture placed at a position 70 cm behind the gas jet. The transmitted-pulse signal was recorded by translating the position z of the laser focus or the focusing lens along the optic axis, as illustrated in Fig. 14. In this configuration, we see above 10% of the area of the incident beam.

Figure 14 shows examples of the result for He, where the laser pulse is propagating from the left to the right, as illustrated at the top. The center of the gas jet or the position $z=0$ was identified as the peak of ion signal observed as a function of z for a low-pressure He at a low laser intensity [see Fig. 15(c)]. When there is no gas jet, as shown in Fig. 14(a), no appreciable change in the pulse signal is observed by translating the laser focus in the range of $z \approx \pm 6$ mm. This constant signal, which is normalized to 10 at each scan in Fig. 14, results from the large focal depth for the small beam area observed. For the 150-Torr He jet, the signal is greatly modulated along z and the modulation increases with increasing I_0, as seen in Figs. 14(b) and 14(c). This modulation certainly demonstrates the defocusing of the laser beam in the ionizing medium and the qualitative interpretation is given as follows.

Let us look at the result shown in Fig. 14(b) and suppose that the laser focus is translated form the left to the right. When the laser focus is far from the gas jet, the laser intensity is too weak to induce a large refractive index change of the medium and resulting defocusing. As the beam waist approaches the gas jet, the laser intensity is increased in the medium and the medium starts to be ionized strongly. When the beam waist is located ($z<0$) in front of the medium, the laser beam going into the medium is significantly diverged by the negative-lens effect of the ionizing medium. This leads to a decrease in the pulse energy transmitted through the aperture. On the other hand, when the beam waist is moved to a position ($z>0$) behind the gas jet, the laser beam slightly converging into the medium is collimated by the negative-lens effect. This results in an increase in the pulse energy to be detected. With a further translation of the beam waist to $z>0$, the signal peaks and then decreases down to the original level due to a decrease in the laser intensity or the medium ionization. A small portion of the incident laser pulse energy is certainly absorbed to ionize the medium, but the absorption never enhances the signal up to or above the original level in vacuum.

To see the effect of defocusing on the harmonic generation, we measured the harmonic signal as a function of z at high intensity. Examples of the results for the 13th and 89th orders generated in He are shown in Figs. 15(a) and 15(b), respectively, together with (c) the ion signal observed, where the signal peak is normalized to 10 at each scan. The 13th-order harmonic is peaked around $z \sim +2.5$ mm where the transmitted laser pulse is collimated and peaked as seen in Fig. 14(c). The collimated beam reduces the peak laser intensity but increases the interaction volume in the medium. This indicates that the 13th-order generation is optimized by a large interaction volume at a relatively low intensity. In contrast to this, the 89th-order harmonic signal is peaked at $z \sim +0.7$ mm, where the defocusing effect is effectively minimized [see Fig. 14(c)]. This suggests that the 89th order is produced most efficiently at the highest intensity achieved on the optic axis. These results demonstrate that a higher intensity is required also in space for the efficient generation of a higher-order harmonic, as shown in time by the blueshift of harmonic spectra. When the laser focus is fixed, the instantaneous yield of different-order harmonics would be peaked at a different part of the interaction volume.

Throughout the present experiments, most data such as the harmonic distributions shown in Fig. 4 have been obtained with the laser focus at $z \sim +0.7$ mm. When the laser focus was translated along z, the harmonic distribution has shown several different characteristics. In comparison with the result shown in Fig. 4, for example, the harmonic distribution observed with the laser focus at $z \sim +2$ mm represented a broader peak around the 19th–25th orders, a faster decrease of the harmonic signal in the plateau with the increase in the harmonic order, a smaller enhancement around

the cutoff, and a faster decrease in the high-order harmonics above the cutoff. These behaviors of harmonics originate from the fact that the defocusing reduces the peak intensity and increases the interaction volume in the gas jet.

The maximum laser intensity achieved in an ionizing medium may be defined as the *interaction intensity* I^*, which must be lower than I_0 and depend on the specific medium and its pressure. This intensity I^* should also be an important parameter to discuss the harmonic generation process in an ionizing medium. The result shown in Fig. 14 may allow us to estimate I^* with respect to the laser focus at z. For this purpose, we make a simple analysis concerning the phase change of a lowest-order Gaussian beam in the ionizing medium. Suppose that the laser beam is focused with a waist radius w_0 at $z=z_0$ and the Gaussian is maintained after passing through the medium. The ultrashort strong laser pulse produces a sharp ionization contour in the medium and then a homogeneous plasma is assumed in the small central beam area to be observed in the z-scan method.

It is well known that the focused Gaussian beam is characterized by the on-axis phase relative to the plane wave. We consider a uniform gas jet located at $z=z_1 \sim z_2$ $(z_1<z_2<z_0)$ in the near field of $|z|<z_R=\pi w_0^2/\lambda$. The refractive index change δn of the medium due to ionization brings about the phase change $\Delta\phi_p=(2\pi/\lambda)L\delta n$ of the incident Gaussian beam, where $L=z_2-z_1$ is the medium length and $\delta n=-\frac{1}{2}\omega_p^2/\omega^2=-\frac{1}{2}(N_e/N_c)$ with the critical density N_c for the laser frequency ω. After passing through the medium, the Gaussian beam has the on-axis phase $\phi_G=-(z-z_0)/z_R+\Delta\phi_p$. This modified phase ϕ_G leads to a change of the far-field divergence angle $\theta\approx\lambda/\pi w_0$ in vacuum and modulates the transmitted pulse signal along z.

In Fig. 14(c), the transmission signal is recovered to the original level at $z_0\sim+0.7$ mm. This shows that the modified far-field divergence angle θ_s due to the defocusing is restored to the original value of θ. This is the case of $\Delta\phi_p=L_0/z_R$, because $\phi_G=-(z-z^*)/z_R-(z^*-z_0)/z_R+\Delta\phi_P$, where $L_0=z_0-z^*$ is a characteristic length shorter than $\sim z_R$. Then, after transmitting the medium, the Gaussian beam propagates as if a new beam waist of the radius w_0 is virtually formed at $z=z^*$. Thus we have

$$N_e/N_c\approx(\lambda/\pi w_0)^2(L_0/L) \tag{13}$$

for the condition of $\theta_s\approx\theta$. With $L_0=L$, Eq. (13) coincides with the relation given by Rankin *et al.* [45] as the condition that the radius of curvature of the incident beam becomes infnite in an ionizing medium.

Similar consideration leads to the relations for defocusing $(\theta_s>\theta)$ and collimating $(\theta_s<\theta)$ the incident beam. We have found that the signal change around $z_0\sim+0.7$ mm in Fig. 14(c) can be reproduced well with $L_0=0.8$–1.5 mm, and then Eq. (13) leads to $N_e/N_0=0.036$–0.068 for the 150-Torr He. Referring to the result shown in Fig. 1, one finds that this small decrease in $N(t)/N_0$ is achieved at $I(t)=(7.3$–$8.0)\times10^{14}$ W/cm^2 in the leading edge of the laser pulse of $I_0\sim3\times10^{15}$ W/cm^2. This value of $I(t)$ corresponds to I^* achieved for the laser focus at $z_0\sim+0.7$ mm in the 150-Torr He. As shown in Fig. 15(b), the 89th-order harmonic is peaked at the same focusing position $z_0\sim+0.7$ mm and the effective intensity I_{89} should be close to this value of I^*. Comparing I^* with I_{15} and I_{29} estimated from the blueshifts, the higher value of I^* shows that the lower orders in the plateau are produced efficiently at lower intensities than I^*.

In the above analysis, it was impossible to apply a single value of L_0 to reproduce the transmitted pulse signal over a distance of more than ~0.5 mm around $z_0=0$, where the signal change observed was much faster than the numerical one. This is due most likely to the facts that N_e is not constant for the different position of laser focus, especially for the position around $z_0=0$, and also would have some different radial distribution depending on the position of laser focus. Furthermore, we suppose that the laser pulse does not maintain the Gaussian distribution in the rapidly ionizing medium. As shown by Rankin *et al.* [45], when N_e tends to exceed the value given by Eq. (13), the laser pulse is modified very quickly after propagating a short distance in the medium, due to the fast phase change. Then the laser intensity $I(t)$ in the medium would be self-regulated to a level of I^* [45,48].

In Fig. 5, the high-order harmonic signals are observed to increase with increasing I_0 up to a value much higher than $I^*\sim8.0\times10^{14}$ W/cm^2. This originates from an increase in the medium volume interacting at $\sim I^*$ rather than an increase in I^* itself. Then the saturation of harmonic signals observed at $I_0>\sim2\times10^{15}$ W/cm^2 is attributed to the saturation of the interaction volume to be observed.

The strong self-defocusing was also observed in Ne. The signal modulation was in almost the same level as that shown in Fig. 14(c) for 18.5-Torr Ne at $I_0\approx3.2\times10^{15}$ W/cm^2, where the modulated signal was restored to the original level at $z\sim+0.2$ mm. This result also shows that Ne atoms are ionized more quickly than He due to the larger ionization rate.

V. DISCUSSION

The theory of harmonic generation in the tunneling regime [17–19,23,39] is mainly concerned with a single-atom response and accounts well for the characteristic behaviors of high-order harmonics such as the formation of a plateau and its sharp cutoff observed. In addition to the single-atom response, the experimental results usually include collective effects such as the phase matching and the competing processes originating from the strong ionization. The characteristic behaviors of harmonics observed and shown in Figs. 4–7 can be discussed qualitatively based on the interaction intensity I^* in the ionizing medium and the effective intensity I_q for the qth-order harmonic generation.

In Fig. 4(a), the harmonic distribution observed at $I_0=7.5\times10^{14}$ W/cm^2 includes a plateau extended up to approximately the 59th order. At this relatively low intensity, only a small medium volume near the optic axis can interact at the peak value I_0 and then the plateau is formed by some low orders that saturate at I_0 or less. In fact, as seen by the blueshift, I_q for the 15th- and 29th-order generation is $(6$–$7)\times10^{14}$ W/cm^2 and never increases at higher values of I_0. With increasing I_0, the medium volume interacting at I_q for the qth-order harmonic in the plateau increases toward the radial direction of the incident beam and then the qth-order

harmonic signal increases to some extent. Simultaneously, some higher orders join the plateau due to the increases in the laser intensity (up to I^*) and in the medium volume interacting at higher intensities, leading to an extension of the plateau to higher orders. With a further increase in I_0 to a value much higher than I^*, the plateau is hardly extended to higher orders owing to the laser intensity limited to I^* in the medium and the saturation of medium volume interacting at I^*. Then the harmonic distribution can no longer change. In the present experiments using 150-Torr He, this complete saturation of the harmonic generation is observed at $I_0 > \sim 2\times 10^{15}$ W/cm^2 with $I^* \sim 8.0\times 10^{14}$ W/cm^2, as shown in Sec. IV. (The laser intensity for the saturation would depend on the experimental configuration to detect the harmonics. If the observed beam area was smaller, the saturation would be observed at a lower value of I_0.)

Thus one can expect that the high orders near the end of a plateau are produced efficiently and saturated at $I_q \sim I^*$ by a laser pulse having $I_0 \gg I^*$. Then some enhancement of these harmonics may be produced through the following process. At $I_0 \gg I^*$, $I(t)$ at time t increases very quickly and reaches $I(t) \sim I^*$ at the beginning of the laser pulse and is self-regulated to $\sim I^*$ in the medium by the rapid ionization and resulting self-defocusing. This gives rise to a rapid saturation of the medium volume interacting at $\sim I^*$, which may be accompanied by an enhancement of the qth-order harmonic produced efficiently at $I_q \sim I^*$. As shown in Figs. 4(a) and 7(a), this would be the case for the 75th–85th orders observed in He at $I_0 \sim 3\times 10^{15}$ W/cm^2. Because of almost the same value of $I_q \sim I^*$ for $q \approx 75$–85, these orders should represent almost the same ε dependence, as seen in Fig. 8(a).

When I_0 is much higher than I^*, the propagation effect for the low orders produced at $I_q < \sim I^*$ is not very important [15,32–34] because of the weak intensity dependence of $d(q\omega)$ and the resulting saturation of harmonic yield. On the other hand, the situation is quite different for the harmonics higher than the plateau end. In Fig. 7, the end of plateau appears to move to higher orders with decreasing the medium pressure. In particular we note in Fig. 7(a) that the signals of harmonics higher than the approximately 85th order are almost independent of the medium pressure ($> \sim 20$ Torr). This characteristic behavior of the higher orders may be illustrated as follows. The dipole moments for these higher orders above the plateau end are not saturated at $\sim I^*$ [23,39], i.e., I_q for these harmonics is higher than I^*. Then the unsaturated harmonic yield would be significantly dominated by the coherence length L_c or the phase mismatch in the medium. In a rapidly ionizing medium, $L_c \sim \pi/\Delta k$, derived from Eq. (6), is a function of the electron density N_e, the harmonic order q, and the confocal parameter b. Because I^* is limited by an absolute value of N_e rather than N_0 or N/N_0 [see Eq. (13)], N_e produced in the medium would be almost constant at different pressures. Then, for constant values of I_0 and b, L_c becomes a simple function decreasing with an increase in the order q. This indicates that the harmonic yield unsaturated at $\sim I^*$ decreases with an increase in the order q, being independent of N_0.

Recently, experimental studies [12,51,52] have been reported for the spatial distributions of harmonic radiation generated in rare gases. At high intensities, the angular divergence of harmonics is found to be almost constant in the plateau and decreases rapidly above the cutoff region with an increase in the harmonic order [12,51]. This has been understood by the intensity-dependent harmonic generation in the nonperturbative regime [51]. We believe that the above discussion based on I^* and I_q is consistent with the previous one and is useful for a detailed understanding of the angular distribution of harmonics.

The maximum harmonic energy $E_{\max}$ predicted by Eq. (11) has often been estimated and discussed in terms of the observed harmonic close to the end of plateau and of the peak laser intensity I_0 used [23,24]. From the above discussion, it is more reasonable in the present experiment to compare $E_{\max}$ with the highest order observed. Furthermore, as in our previous experiment, where we had strong multiphoton ionization of atoms with the femtosecond uv laser pulses [11], I^* in the medium must be used to estimate $E_{\max}$. Using $I^* \sim (7.3$–$8.0)\times 10^{14}$ W/cm^2 obtained at $I_0 > \sim 2\times 10^{15}$ W/cm^2 for the 150-Torr He, we have $E_{\max} \approx 157$–169 eV. This corresponds to the 99th- to 107th-order harmonic energy at $\lambda \sim 782$ nm and is in good agreement with that of the 103rd order observed.

For the generation of higher-order harmonics or shorter-wavelength coherent radiation, a higher value of I^* has to be achieved in the medium. One of the most effective approaches is to shorten the laser pulse width.

VI. CONCLUSION

Using femtosecond high-intensity Ti:sapphire laser pulses, we have performed a systematic study of high-order harmonic generation in He and Ne at laser intensities up to $I_0 \sim 3\times 10^{15}$ W/cm^2. The main results obtained are summarized as follows.

(i) The highest orders (shortest wavelengths) observed are the 103rd (7.6 nm) in He and the 95th (8.2 nm) in Ne. The harmonic distribution observed at the highest intensity represents a broad plateau that includes a peak at low orders around the atomic ionization potential and an enhancement at the end of the plateau.

(ii) It has been observed that the harmonic yield of high orders located above the plateau is almost independent of the medium pressure. This is attributed to the saturation of the interaction intensity I^* in the rapidly ionizing medium.

(iii) The laser-ellipticity dependences strongly suggest that the high-order harmonics in and above the plateau are generated through tunneling, while the low orders below and around the atomic ionization potential are predominantly produced by the nonlinear response of atomic electrons.

(iv) The effective intensity I_q for the qth-order harmonic generation has been estimated by observing blueshifts of harmonic spectra and is found to be almost constant at $I_0 \gg I_q$.

(v) Effects of self-defocusing on the harmonic generation have been studied using the modified z-scan method. The defocusing induced in the ionizing medium is demonstrated to limit the laser intensity to a value I^* much lower than I_0.

(vi) From the measurements of self-defocusing and blueshifts, the generation of a higher-order harmonic is confirmed to require a higher intensity in time and space.

(vii) The characteristic harmonic behaviors observed in the intensity-, pressure-, and ellipticity-dependent generation

are understood well by taking into account I^* in the ionizing medium and I_q for the qth-order harmonic.

(viii) The highest order of harmonics generated is in good agreement with that predicted by the cutoff law, when I^* is used to estimate $E_{\max}$.

ACKNOWLEDGMENTS

The authors would like to thank K. Torizuka and H. Sakai for their help in the early stages of the experiments and P. B. Corkum for his discussion on the ellipticity-dependent harmonic generation.

[1] M. Ferray, A. L'Huillier, X. F. Li, L. A. Lompré, G. Mainfray, and C. Manus, J. Phys. B **21**, L31 (1988); X. F. Li, A. L'Huillier, M. Ferray, L. A. Lompré, and G. Mainfray, Phys. Rev. A **39**, 5751 (1989).

[2] N. Sarukura, K. Hata, T. Adachi, R. Nodomi, M. Watanabe, and S. Watanabe, Phys. Rev. A **43**, 1669 (1991).

[3] K. Miyazaki and H. Sakai, J. Phys. B **25**, L83 (1992); Optoelectronics **8**, 231 (1993).

[4] Ph. Balcou, C. Cornaggia, A. S. L. Gomes, L. A. Lompré, and A. L'Huillier, J. Phys. B **25**, 4467 (1992).

[5] J. K. Crane, M. D. Perry, S. M. Herman, and R. W. Falcone, Opt. Lett. **17**, 1256 (1992).

[6] Y. Akiyama, K. Midorikawa, Y. Matsunawa, Y. Nagata, M. Obara, H. Tashiro, and K. Toyoda, Phys. Rev. Lett. **69**, 2176 (1992); S. Kubodera, Y. Nagata, Y. Akiyama, K. Midorikawa, M. Obara, H. Tashiro, and K. Toyoda, Phys. Rev. A **48**, 4576 (1993).

[7] J. J. Macklin, J. D. Kmetec, and C. L. Gordon III, Phys. Rev. Lett. **70**, 766 (1993).

[8] A. L'Huillier and Ph. Balcou, Phys. Rev. Lett. **70**, 774 (1993).

[9] K. Kondo, N. Sarukura, K. Sajiki, and S. Watanabe, Phys. Rev. A **47**, R2480 (1993).

[10] M. D. Perry and J. K. Crane, Phys. Rev. A **48**, R4051 (1993).

[11] K. Miyazaki, H. Sakai, G.U. Kim, and H. Takada, Phys. Rev. A **49**, 548 (1994).

[12] J. G. W. Tisch, R. A. Smith, J. E. Muffett, M. Ciarrocca, J. P. Marangos, and M. H. R. Hutchinson, Phys. Rev. A **49**, R28 (1994); J. G. W. Tisch, J. E. Muffett, R. A. Smith, M. Ciarrocca, J. P. Marangos, M. H. R. Hutchinson, and C. G. Wahlstrom, in *Multiphoton Processes,* edited by D. K. Evans and S. L. Chin (World Scientific, Singapore, 1994), p. 215.

[13] K. Miyazaki, H. Takada, K. Torizuka, and H. Sakai, in *Multiphoton Processes* (Ref. [12]), p. 241.

[14] J. L. Krause, K. J. Schafer, and K. C. Kulander, Phys. Rev. Lett. **68**, 3535 (1992).

[15] A. L'Huillier, K. J. Schafer, and K. C. Kulander, J. Phys. B **24**, 3315 (1991), and references therein.

[16] K. J. Schafer, J. L. Krause, and K. C. Kulander, Int. J. Nonlinear Opt. Phys. **1**, 245 (1992), and references therein.

[17] P. B. Corkum, Phys. Rev. Lett. **71**, 1994 (1993).

[18] K. J. Schafer, B. Yang, L. F. DiMauro, and K. C. Kulander, Phys. Rev. Lett. **70**, 1599 (1993).

[19] K. C. Kulander, K. J. Schafer, and J. K. Krause, in *Super-Intense Laser-Atom Physics*, edited by B. Piraux *et al.* (Plenum, New York, 1993), p. 95.

[20] K. S. Budil, P. Salieres, A. L'Huillier, T. Ditnire, and M. D. Perry, Phys. Rev. A **48**, R3437 (1993).

[21] P. Dietrich, N. H. Burnett, M. Ivanov, and P. B. Corkum, Phys. Rev. A **50**, R3585 (1994).

[22] N. H. Burnett, C. Kan, P. B. Corkum, and M. Ivanov (unpublished).

[23] A. L'Huillier, M. Lewenstein, P. Salieres, Ph. Balcou, M. Yu. Ivanov, J. Larsson, and C. G. Wahlström, Phys. Rev. A **48**, R3433 (1993).

[24] C. G. Wahlström, J. Larsson, A. Persson, T. Starczewski, S. Svanberg, P. Salieres, Ph. Balcou, and A. L'Huillier, Phys. Rev. A **48**, 4709 (1993).

[25] S. C. Rae and K. Burnett, Phys. Rev. A **48**, 2490 (1993).

[26] S. C. Rae and K. Burnett, J. Phys. B **26**, 1509 (1993).

[27] L. V. Keldysh, Zh. Éksp. Teor. Fiz. **47**, 1945 (1964) [Sov. Phys. JETP **20**, 1307 (1965)].

[28] M. V. Ammosov, N. B. Delone, and V. P. Krainov, Zh. Éksp. Teor. Fiz. **91**, 2008 (1986) [Sov. Phys. JETP **64**, 1191 (1986)]; M. V. Ammosov, P. A. Golovinsky, I. Yu. Kiyan, V. P. Krainov, and V. M. Ristic, J. Opt. Soc. Am. B **9**, 1225 (1992).

[29] S. Augst, D. Strickland, D. D. Meyerhofer, S. L. Chin, and J. H. Eberly, Phys. Rev. Lett. **63**, 2212 (1989); S. Augst, D. Strickland, D. D. Meyerhofer, and S. L. Chin, J. Opt. Soc. Am. B **8**, 858 (1991).

[30] F. A. Ilkov, J. E. Decker, and S. L. Chin, J. Phys. B **25**, 4005 (1992).

[31] See, e.g., J. F. Reintjes, *Nonlinear Optical Parametric Processes in Liquids and Gases* (Academic, London, 1984), p. 155.

[32] A. L'Huillier, K. J. Schafer, and K. C. Kulander, Phys. Rev. Lett. **66**, 2200 (1991).

[33] A. L'Huillier, Ph. Balcou, S. Candel, K. J. Schafer, and K. C. Kulander, Phys. Rev. A **46**, 2778 (1992).

[34] Ph. Balcou and A. L'Huillier, Phys. Rev. A **47**, 1447 (1993).

[35] Y. Liang, M. V. Ammosov, and S. L. Chin, J. Phys. B **27**, 1269 (1994).

[36] See, e.g., R. R. Freeman and P. H. Bucksbaum, J. Phys. B **24**, 325 (1991).

[37] H. Xu, X. Tang, and P. Lambropoulos, Phys. Rev. A **46**, R2225 (1992).

[38] N. H. Burnett, C. Kan, and P. B. Corkum, Phys. Rev. A **51**, R3418 (1995).

[39] M. Lewenstein, Ph. Balcou, M. Yu. Ivanov, A. L'Huillier, and P. B. Corkum, Phys. Rev. A **49**, 2117 (1994).

[40] W. Becker, S. Long, and J. K. McIver, Phys. Rev. A **50**, 1540 (1994), and references therein.

[41] E. Yablonovitch, Phys. Rev. Lett. **60**, 795 (1988).

[42] W. M. Wood, C. W. Siders, and M. C. Downer, Phys. Rev. Lett. **67**, 3523 (1991); B. M. Penetrante, J. N. Bardsley, W. M. Wood, C. W. Siders, and M. C. Downer, J. Opt. Soc. Am. B **9**, 2032 (1992).

[43] S. P. Le Blanc, R. Sauerbrey, S. C. Rae, and K. Burnett, J. Opt. Soc. Am. B **10**, 1801 (1993).

[44] S. C. Rae, K. Burnett, and J. Cooper, Phys. Rev. A **50**, 3438 (1994).

[45] R. Rankin, C. E. Capjack, N. H. Burnett, and P. B. Corkum, Opt. Lett. **16**, 835 (1991).
[46] W. P. Leemans, C. E. Clayton, W. B. Mori, K. A. Marsh, P. K. Kaw, A. Dyson, and C. Joshi, Phys. Rev. A **46**, 1091 (1992).
[47] P. Monot, T. Auguste, L. A. Lompré, G. Mainfray, and C. Manus, J. Opt. Soc. Am. B **9**, 1579 (1992).
[48] S. C. Rae, Opt. Commun. **97**, 25 (1993).
[49] H. Sakai and K. Miyazaki, Phys. Rev. A **50**, 4204 (1994).
[50] See, e.g., M. S. Bahae, A. A. Said, T.-H. Wei, D. J. Hagan, and E. W. van Strayland, IEEE J. Quantum Electron. **26**, 760 (1990); W. Zhao and P. P. Muhoray, Appl. Phys. Lett. **63**, 1613 (1993).
[51] P. Salieres, T. Ditmire, K. S. Budil, M. D. Perry, and A. L'Huillier, J. Phys. B **27**, L217 (1994).
[52] D. D. Meyerhofer and J. Peatross, *Multiphoton Processes* (Ref. [12]), p. 409.